

Discovering a Defect that Limits Mg Doping in p-Type GaN

Z. Liliental-Weber, T. Tomaszewicz, D. Zakharov and M.A. O'Keefe

Materials Sciences Division, Lawrence Berkeley National Laboratory, Berkeley, CA 94720, USA

Gallium nitride (GaN) is the III-V semiconductor used to produce blue light-emitting diodes (LEDs) and blue and ultraviolet solid-state lasers. To be useful in electronic devices, GaN must be doped with elements that function either as electron donors or as acceptors to turn it into either an n-type semiconductor or a p-type semiconductor. It has been found that GaN can easily be grown with n-conductivity, even up to large concentrations of donors – in the few 10^{19}cm^{-3} range. However, p-doping, the doping of the structure with atoms that provide electron sinks or holes, is not well understood and remains extremely difficult. The only efficient p-type dopant is Mg, but it is found that the free hole concentration is limited to $2 \times 10^{18}\text{cm}^{-3}$, even when Mg concentrations are pushed into the low 10^{19}cm^{-3} range. This saturation effect could place a limit on further development of GaN based devices. Further increase of the Mg concentration, up to $1 \times 10^{20}\text{cm}^{-3}$ leads to a decrease of the free hole concentration and an increase in defects. While low- to medium-brightness GaN light-emitting diodes (LEDs) are remarkably tolerant of crystal defects, blue and UV GaN lasers are much less so. We used electron microscopy to investigate Mg doping in GaN.

Our transmission electron microscopy (TEM) studies revealed the formation of different types of Mg-rich defects [1,2]. In particular, high-resolution TEM allowed us to characterize a completely new type of defect in Mg-rich GaN. We found that the type of defect depended strongly on crystal growth polarity. For crystals grown with N-polarity, planar defects are distributed at equal distances (20 unit cells of GaN); these defects can be described as inversion domains [1]. For growth with Ga-polarity, we found a different type of defect [2]. These defects turn out to be three-dimensional Mg-rich hexagonal pyramids (or trapezoids) with their base on the (0001) plane and their six walls formed on $\{11\bar{2}3\}$ planes (Fig. 1a). In $[11\bar{2}0]$ and $[1\bar{1}00]$ cross-section TEM micrographs the defects appear as triangular (Fig. 1b) and trapezoidal (Fig. 1c). In projection, the sides of these defects are inclined at 43° and 47° to the base depending on the observation direction. The pyramid size varies from 50\AA - 1000\AA depending on the growth method, but the angle between the base and sides remain the same. The direction from the tip of the pyramid to its base (and from the shorter to the longer base for trapezoidal defects) is along the Ga to N matrix bond direction (Fig. 1a-d).

To obtain adequate atomic resolution, we used software correction of microscope aberrations by recording focal-series of images and using them to reconstruct the electron exit-surface wave (ESW) as it left the specimen. Phase changes experienced by the electron wave traversing the specimen form a record of the spatial distribution of its potential (i.e., the positions of the atoms). For a plane wave incident on the specimen, the phase of the ESW is a map of the atom positions. Although the resolution with which a microscope can convert the ESW into an image is limited by microscope aberrations (notably C_s), a well-chosen focal series can contain phase information out to the microscope information limit. This “extra” high-resolution information can be retrieved by focal-series reconstruction to remove the resolution-limiting lens aberrations [3]. Because phase change is proportional to scattering power, one can distinguish between different elements contributing to the retrieved phase. Heavier atoms produce more phase change – in GaN the phase change produced by a Ga atom column is always stronger than the phase change produced by a N column with the equivalent number of atoms. With increasing numbers of atoms in the columns (increasing thickness), the phase change moves to produce a counterclockwise Argand plane trajectory of the complex ESW vector at the atom position [4]. Since the phase change for Ga is much faster than for N for the same number of atoms in the column, we can distinguish between Ga and N columns and determine the crystal thickness and polarity. Because projected Ga-N distances are 1.13\AA , we used the CM300-OAM [5] with a corrected resolution of up to 0.78\AA [6] to record our images.

Reconstructed exit wave phase from the area close to the pyramid tip showed maxima with two distinct intensity peaks. Using Argand plots, we confirmed that the phase of atoms described as Ga gave the highest peak, followed by a smaller phase peak identified as N (Figs. 1 e-h). This identification of the atomic positions of Ga and N from the experimental reconstructed exit wave confirmed inversion of polarity within the pyramid compared to the matrix. In addition, it showed that AB stacking in the matrix changes to BC stacking within the pyramid. This stacking arrangement holds through the entire pyramid and changes back to the AB stacking order above the pyramid base. Analysis of the reconstructed exit wave phase image from the pyramid side (Fig. 1e,f) indicates a shift of Ga atomic column positions from the matrix to the N position within the pyramid. Detailed analysis reveals that the walls of the pyramid are covered with Mg atoms. Because Mg atoms prefer to accumulate on $\{11\bar{2}3\}$ planes, they end up building pyramids that act as traps, removing Mg from the matrix and from its “job” of functioning as a p-type dopant [7].

- [1] Z. Liliental-Weber, et al, *Phys. Rev. Lett.* **82**, 2370 (1999).
 [2] Z. Liliental-Weber, et al, *Phys. Rev. Lett.* **93**, 206102 (2004);
 [3] A. Thust, et al, *Ultramicroscopy* **64**, 211 (1996).
 [4] W. Sinkler and L. D. Marks *Ultramicroscopy* **75**, 251 (1999).
 [5] M.A. O’Keefe et al. *Ultramicroscopy* **89**, (2001) 215.
 [6] M.A. O’Keefe & L.F. Allard, *Microscopy & Microanalysis* **10** (2004) 1002-1003.
 [7] Supported by Office of Science, Office of Basic Energy Sciences, Materials Science & Engineering Division, DOE, under contract DE-AC03-76SF00098.

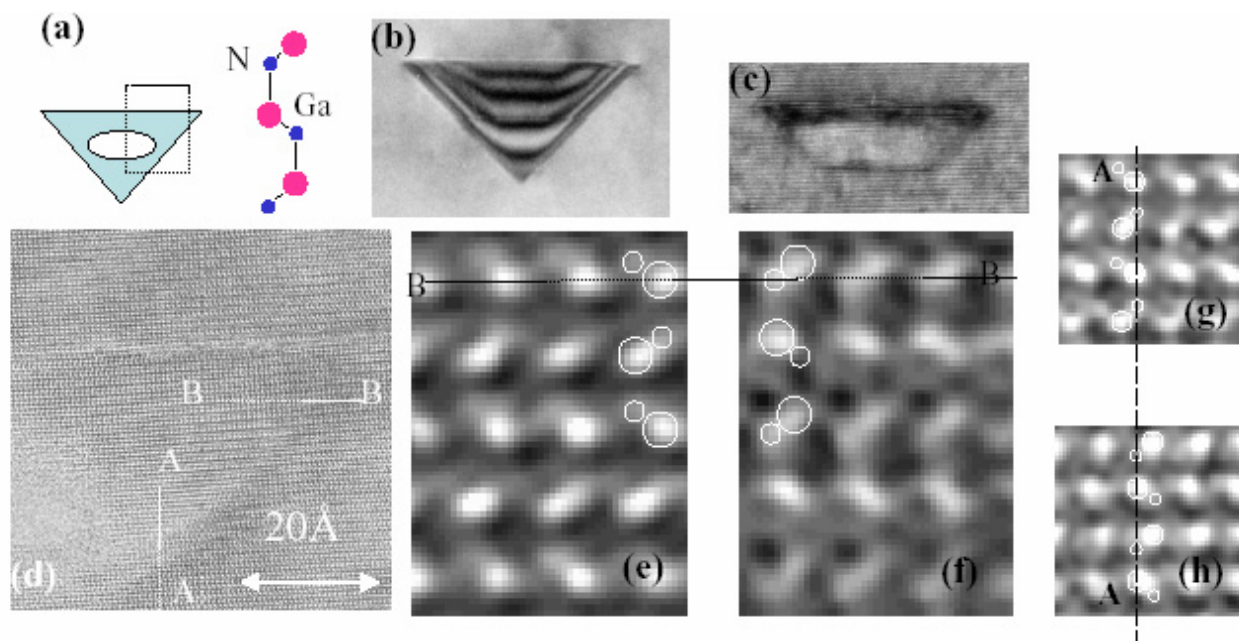


FIG. 1. (a) Schematic of pyramidal defect with outlined part shown in high resolution in (d). A hole formed inside the pyramid {proved experimentally in (d)} is also shown. Ga matrix polarity is indicated as well as arrangement of defects (b), (c) and (d) in this matrix; (b) and (c) Cross section of pyramidal and trapezoidal defects, respectively; (d) Cross-section image from the part of a pyramid {outlined in (a)}; (e) and (f) reconstructed exit wave phase from the side of the pyramid/matrix interface along the B-B line shown in (d): (e)-inside the pyramid, (f)-the matrix outside the pyramid, (g) and (h) reconstructed exit wave phase from the pyramid/matrix interface along the A-A line shown in (d); (e) inside the pyramid and (h) in the matrix below the pyramid aligned along c-axis. Note stacking change within the defect (BC) compared to the matrix (AB).